

Solitons and Physics of the Lysogenic to Lytic Transition in Enterobacteria Lambda Phage

Andrei Krokhotin¹ and Antti J. Niemi^{2,1}

¹*Department of Physics and Astronomy, Uppsala University, P.O. Box 803, S-75108, Uppsala, Sweden*

²*Laboratoire de Mathématiques et Physique Théorique CNRS UMR 6083,*

Fédération Denis Poisson, Université de Tours, Parc de Grandmont, F37200, Tours, France

The lambda phage is a paradigm temperate bacteriophage. Its lysogenic and lytic life cycles echo competition between the DNA binding CI and CRO proteins. Here we address the Physics of this transition in terms of an energy function that portrays the backbone as a multi-soliton configuration. The precision of the individual solitons far exceeds the B-factor accuracy of the experimentally determined protein conformations giving us confidence to conclude that three of the four loops are each composites of two closely located solitons. The only exception is the repressive DNA binding turn, it is the sole single soliton configuration of the backbone. When we compare the solitons with the Protein Data Bank we find that the one preceding the DNA recognition helix is unique to the CI protein, prompting us to conclude that the lysogenic to lytic transition is due to a saddle-node bifurcation involving a soliton-antisoliton annihilation that removes the first loop.

The CI repressor protein and its lytic counterpart, the CRO protein of the Escherichia coli binding λ phage, are among the most extensively studied proteins in molecular biology [1], [2]. They display a highly intriguing biological behavior by controlling the transitions between the lysogenic and lytic phases, that has been detailed in numerous molecular biology textbooks and review articles. At a qualitative, mechanistic level the transition between the lysogenic and lytic phases is quite well understood [1], [2]. But at a quantitative level we do not yet understand the physical principle that triggers the transition. Since lysogeny is an important example of gene control by repressors, a quantitative Physics based explanation should have wide biophysical interest and applicability.

In this Letter we search for a Physics based explanation for the transition between lysogenic and lytic phases in the λ phage. For this we scrutinize the fine structure of the folded CI repressor protein, a homo-dimer with 92 residues in each of the two monomers [1]. The protein binds to DNA with a helix-turn-helix motif that is located between the residue sites 33-51. Full crystallographic information is available in Protein Data Bank (PDB) under code 1LMB.

We construct the 1LMB backbone conformation explicitly in terms of solitons that emerge as classical solutions to the following energy function [3]-[6],

$$E = - \sum_{i=1}^{N-1} 2\kappa_{i+1}\kappa_i + \sum_{i=1}^N \{2\kappa_i^2 + c \cdot (\kappa_i^2 - m^2)^2\} + \sum_{i=1}^N \{b\kappa_i^2\tau_i^2 + d\tau_i + e\tau_i^2\} \quad (1)$$

The summation extends over all residues with $\kappa_i \in [-\pi, \pi] \bmod(2\pi)$ the bond angle along the lattice that is formed by the central C_α carbons, and $\tau_i \in [-\pi, \pi] \bmod(2\pi)$ the ensuing torsion angle. The parameters (c, m, b, d, e) are all global and specific to a given motif. Once these angles are known, we can use the discrete Frenet equation to reconstruct the protein backbone as a piecewise linear polygonal chain.

We emphasize that the energy function (1) does not purport to explain the details of the atomary level mechanisms that fold the CI protein. Rather, it enables us to examine the properties of the folded CI in terms of universal physical arguments.

Curiously, (1) has the functional form of the discretized Landau-Ginzburg free energy, that similarly describes the Physics of superconductivity [7]: In a continuum limit the first two terms of (1) combine into derivative of curvature that plays the rôle of Cooper pair density in the Landau-Ginzburg theory. The third term is the symmetry breaking potential. The fourth term has its origin in spontaneous symmetry breaking, its presence leads to the notorious Meissner effect in superconductivity [7]. The fifth term which is absent in the standard Landau-Ginzburg free energy, is the Chern-Simons term that gives the protein backbone its chirality. Finally, the last term is like the Proca mass of a supercurrent. In fact, in (1) we have included *exactly* all those terms that are consistent with general principles of universality and gauge invariance [3].

We start by introducing the classical equations of motion for (1). We first eliminate τ_i in terms of the bond angles

$$\frac{\partial E}{\partial \tau_i} = 2b\kappa_i^2\tau_i + 2e\tau_i + d = 0 \Rightarrow \tau_i[\kappa_i] = -\frac{1}{2} \cdot \frac{d}{e + b\kappa_i^2} \equiv -\frac{1}{2} \cdot \frac{1}{\frac{e}{d} + \frac{b}{d} \cdot \kappa_i^2} \quad (2)$$

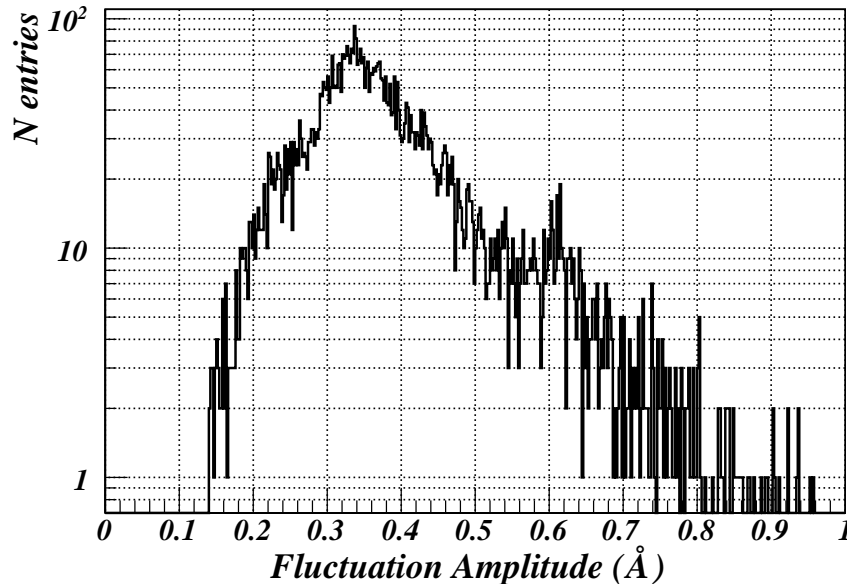


FIG. 1: The number of entries in PDB with temperature below 50K *vs.* Debye-Waller fluctuation distance.

Consequently the torsion angles are determined entirely by the bond angles and the two parameter ratios. When we substitute (2) to the equation for κ_i , we arrive at

$$\kappa_{i+1} - 2\kappa_i + \kappa_{i-1} = U'[\kappa_i]\kappa_i \equiv \frac{dU[\kappa]}{d\kappa_i^2} \kappa_i \quad (i = 1, \dots, N) \quad (3)$$

(with $\kappa_0 = \kappa_{N+1} = 0$) where

$$U[\kappa] = -\frac{d}{2} \cdot \tau[\kappa] - 2cm^2 \cdot \kappa^2 + c \cdot \kappa^4 \quad (4)$$

Since the torsion angle depends only on the parameter ratios $\frac{e}{d}$ and $\frac{b}{d}$, if we scale d , e and b equally the profile of $\tau[\kappa]$ remains intact. In the limit where d becomes vanishingly small the first term in (4) can then be safely removed, and the equation reduces to the ubiquitous spontaneously broken discrete nonlinear Schrödinger equation [8]. Thus, in the $d \rightarrow 0$ limit the solution approaches the soliton profile of the ensuing continuum equation [5],

$$\kappa_i = (-1)^{r+1} \frac{m_{r1} \cdot e^{c_{r1}(i-s_r)} - m_{r2} \cdot e^{-c_{r2}(i-s_r)}}{e^{c_{r1}(i-s_r)} + e^{-c_{r2}(i-s_r)}} \quad (5)$$

Here r labels the different helix-loop-helix motifs of 1LMB, and $(c_{r1}, c_{r2}, m_{r1}, m_{r2}, s_r)$ are specific to the motif; the parameter s_r that is absent in (1) specifies the location of the r th loop. The parameters (c_{r1}, c_{r2}) characterize the length of the loop, and (m_{r1}, m_{r2}) together with the ratios $(\frac{e}{d}, \frac{b}{d})_r$ determine the global character of the helices and strands that are adjacent to the loops. Remarkably this leaves us with *no other* loop specific parameters besides the c_r that determine the length of the loops, and s_r that determine their positions.

We propose that as such the classical soliton profiles are duly describing the C_α lattice only in the limit where thermal fluctuations vanish. But even near zero temperature the protein remains subject to residual zero-point fluctuations. It is difficult to estimate and even harder to accurately calculate the amplitude of these zero-point fluctuations. As a consequence, in order to get a realistic order of magnitude estimate we have inspected the distribution of the B-factors that characterize experimental uncertainties, for all PDB structures where the crystallographic measurements have been made at temperatures less than 50K. The result is displayed in Figure 1. From it we conclude that for the C_α carbons the zero point fluctuations have an amplitude somewhere in the vicinity of the lower bound which is around 0.15 Å. Consequently we describe the estimated range of zero point fluctuations around our classical soliton profiles by dressing them with a tubular dominion that has a radius of 0.15 Å.

TABLE I: Parameter values for each of the seven solitons in Figure 2.

Soliton	c_1	c_2	m_1	m_2	s	e/d	b/d
1	2.00441	1.99595	26.65124	26.68412	24.50259	$-9.9921 \cdot 10^{-2}$	$4.2191 \cdot 10^{-5}$
2	2.94889	2.95201	70.67882	70.60369	30.49642	$-1.5114 \cdot 10^{-7}$	$1.0662 \cdot 10^{-11}$
3	2.89729	2.90755	39.27387	39.22546	41.39325	$-5.3794 \cdot 10^{-7}$	$7.4566 \cdot 10^{-11}$
4	2.97927	3.00015	1.07948	1.52942	53.67225	$5.1477 \cdot 10^{-7}$	$-5.1529 \cdot 10^{-7}$
5	2.96486	2.97087	26.69087	26.25280	57.85123	$-9.62942 \cdot 10^{-8}$	$1.45097 \cdot 10^{-12}$
6	2.94948	2.94547	20.43071	20.38220	70.22069	$-9.27151 \cdot 10^{-7}$	$3.05202 \cdot 10^{-10}$
7	2.89725	2.89945	89.50870	89.55252	75.56315	$-7.13705 \cdot 10^{-7}$	$1.8457 \cdot 10^{-11}$

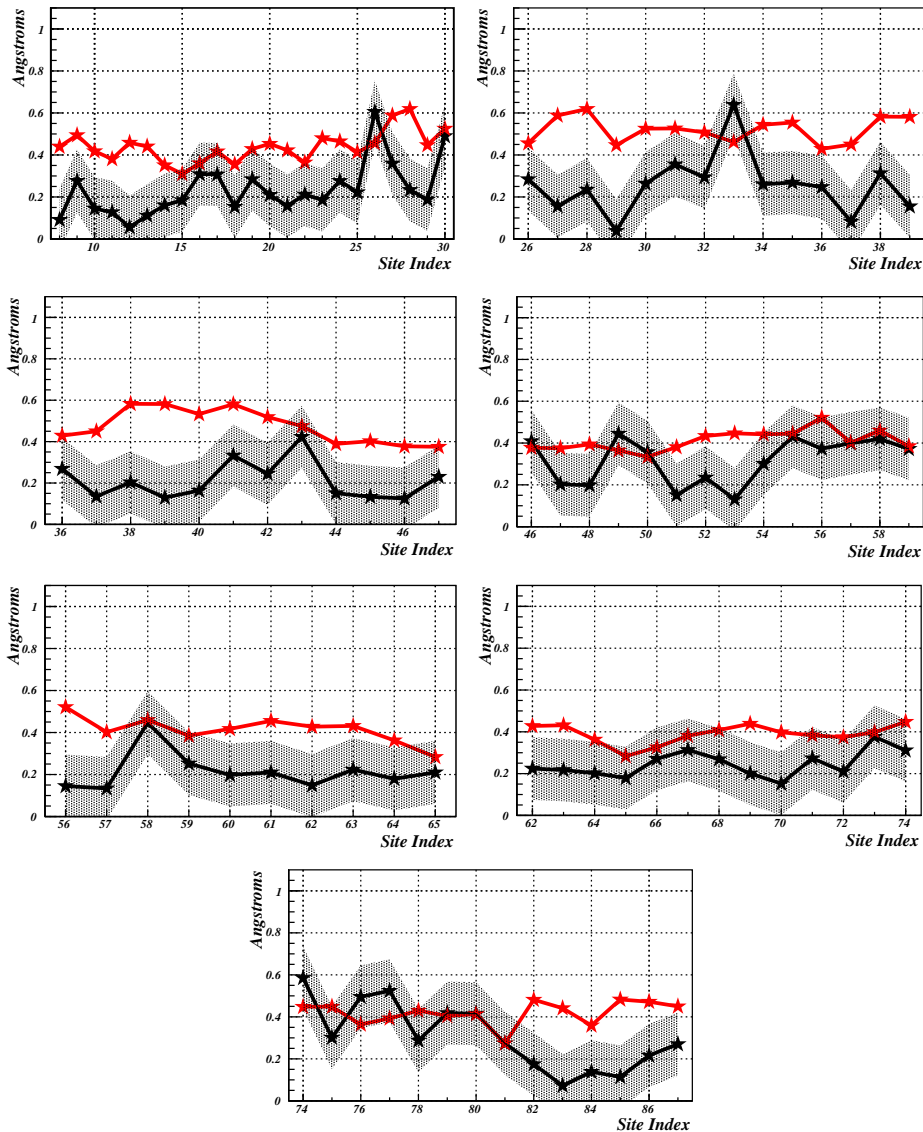


FIG. 2: The seven solitons for the first monomer of 1LMB, with their respective residue numbers. The black line denotes the distance between soliton and corresponding PDB configuration. The red line denotes the Debye-Waller distance that is computed from the B-factors in PDB. The grey area describes the estimated 0.15 Å zero point fluctuation distance of the soliton.

In Table 1 we provide the parameter values for (2) and (5), computed from the PDB data of 1LMB using a Monte

Carlo fitting algorithm. In Figure 2 we compare the ensuing solitons with the folded 1LMB: The solitons describe the structural motifs of 1LMB with a precision that is *substantially* better than the experimental accuracy determined by B-factors, even when we account for the 0.15 Å estimate of the solitons zero point fluctuations.

With the aid of our high accuracy solitons we conclude that in 1LMB there are a total of *seven* α -helices and *one* β -strand. But two of the α -helices and the sole β -strand are so short that until now they have been interpreted as parts of loops. They become exposed only by the high accuracy of our construction. This refinement of the consensus interpretation has important *fully testable* repercussions to the CI protein that allow us to address the Physics of the lysogenic to lytic transition:

The only motif where our soliton picture identifies a loop as a single isolated soliton is the DNA binding one. All of the remaining three putative loops consist of a soliton-antisoliton pair, with the solitons separated from each other either by a *very* short α -helix in case of the residues (23, 33) and (69, 90), or by a *very* short β -strand in case of residues (51, 61). This interpretation reveals itself only when we scrutinize the fine details of the (κ_i, τ_i) spectrum in terms of our solitons. As an example, in Figure 3 we display the putative first helix-loop-helix motif and for comparison we

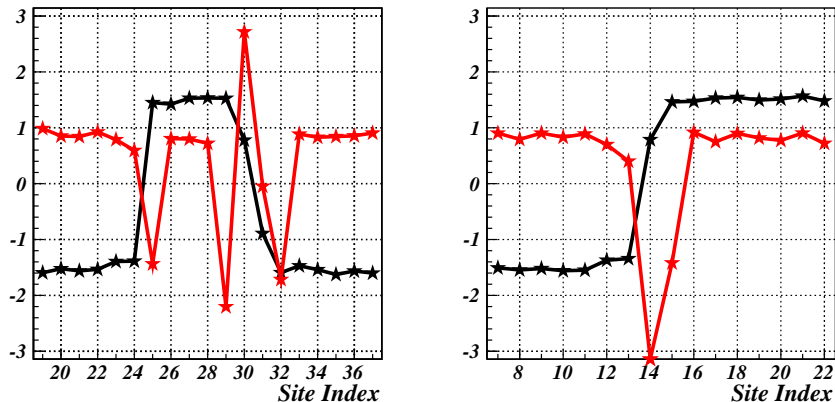


FIG. 3: The resolved (κ_i, τ_i) spectrum for the putative first helix-loop-helix of 1LMB (left) and the corresponding structure of in 2OVG (right). The bond angle κ is black, torsion angle τ is red. The bond angle spectra reveal that in 1LMB the loop is a bound state of two solitons, while in 2OVG there is only one soliton.

display the corresponding structure in the CRO protein with PDB code 2OVG. Our refined interpretation is palpable, in the case of CI the motif is clearly a bound state of two solitons while in the case of CRO we have a single isolated soliton:

The parameter s_r in (5) determines the center of soliton *i.e.* the position of the inflection point in the ensuing space curve where the interpolated bond angle in Figure 3 vanishes. An isolated inflection point such as the one in the right hand side of Figure 3 (2OVG) is topologically stable in the sense that it can not be created nor removed by any continuous local deformation. For a given finite length curve, an individual inflection point *i.e.* a soliton can be made or deleted only by transporting it through one of the end points of the curve. On the other hand, a pair of inflection points *i.e.* a soliton-antisoliton pair such as the one in the left hand side of Figure 3 (1LMB) is not topologically stable but can be created or removed locally by a saddle-node bifurcation that brings the two inflection points together.

A comparison between the CI and CRO soliton profiles in Figure 3 then proposes the following *experimentally fully testable* mechanism for the lysogenic-lytic transition: Under lysogenic conditions where the CI protein prevails, the soliton-antisoliton pairs of the CI protein that are located immediately prior and after the DNA binding domain are relatively stable. But when there is a change in the environmental conditions that excites phonon fluctuations along the protein chain, such as raise in temperature or UV radiation, either of these soliton-antisoliton pairs can discharge by a saddle-node bifurcation. This bifurcation disturbs the structure of the immediately adjacent DNA binding motif to the extent that the protein loses its capability to maintain the lysogenic phase. Since each of the corresponding motifs in the CRO protein are topologically stable single solitons they are insensitive to local phonon excitations, and the lytic phase takes over.

We note that the shoulder of the short α -helix in the last loop is anchored by the presence of a proline at site 78. Consequently in the first approximation we can safely exclude a bifurcation instability from occurring in the putative helix-loop-helix motif between the residues (69, 90).

We still need to conclude which of the two motifs of CI that are adjacent to the DNA binding domain is the one that loses its stability in the proposed bifurcation transition. Unfortunately, it appears that a full answer must wait until computational methods have reached sufficient maturity [9]. However, to provide the probable answer we have performed a statistical analysis on the occurrence of our seven solitons in all PDB proteins. In Table 2 we list

TABLE II: The soliton sites used in searching for matching structures in PDB, together with the number of matches. The search is limited to those x-ray structures that have a resolution better than 2.0 Å and a match is a configuration that deviate less than 0.5 Å in total RMSD distance from the soliton.

Soliton	1	2	3	4	5	6	7
Sites	(20,28)	(27,36)	(36,46)	(50,58)	(55,63)	(66,75)	(74,82)
Matches	9601	4	810	159	1552	1342	406

the number of matches that each of these soliton has when we search PDB for configurations that deviate from the given soliton by an overall RMSD distance less than 0.5 Å. We have chosen this cut-off value since it is representative of the Debye-Waller fluctuation distance in the experimental 1LMB data. The *remarkable* observation is that for the second soliton in the loop preceding the DNA recognition helix, the *only* matching structures are located in the different PDB entries of the λ phage CI protein itself. This absence of the second soliton in PDB *strongly* proposes that the ensuing loop must be unstable when the protein is in any other *in vivo* environment. Thus the most probable source of the lysogenic to lytic transition is the saddle-node bifurcation that takes place in the first loop and makes its soliton-antisoliton pair to annihilate each other. The bifurcation causes the ensuing structure to act like a crowbar that lifts the recognition helix from its place in the DNA groove. We note that *as such*, it is obvious from (1) that in isolation the first soliton-antisoliton pair has an energy which is higher than that of the ground state *i.e.* an α -helix. But a more detailed molecular dynamics simulation needs to be performed to confirm our proposal.

All of the other solitons are ubiquitous in PDB and except for the turn that participates directly to the regulatory process their biophysical rôle remains to be clarified.

Finally, our soliton interpretation reveals the following *fully testable* pattern for the folding pathways of 1LMB: The functionally pertinent DNA binding loop is an isolated soliton, while all the remaining three loop structures consist of a soliton-antisoliton pair. Since an isolated soliton is topologically stable while soliton-antisoliton pairs are not, the DNA binding loop must be created very early, presumably during translation. The initial configuration for the folding process is then a single soliton state. During the folding process the remaining three motifs are created by local phononic fluctuations, as soliton-antisoliton pairs. Due to the presence of the proline at site 78, the ensuing motif probably emerges very early.

A.N. thanks H. Frauenfelder and G. Petsko for communications and J. Åqvist for discussions.

-
- [1] M. Ptashne, A Genetic Switch, Third Edition, Phage Lambda Revisited. Cold Spring Harbor Laboratory Press, Cold Spring Harbor (2004)
- [2] M.E. Gottesman and R.A. Weisberg, Microbiol. Mol. Biol. Rev. **68** 796 (2004)
- [3] A.J. Niemi, Phys. Rev. **D67** 106004 (2003)
- [4] U.H. Danielsson, M. Lundgren and A.J. Niemi, Phys. Rev. **E82** 021910 (2010)
- [5] M. Chernodub, S. Hu and A.J. Niemi, Phys. Rev. **E82** 011916 (2010)
- [6] N. Molkenthin, S. Hu and A.J. Niemi, Phys. Rev. Lett. **106** 078102 (2011)
- [7] P.G. de Gennes, Superconductivity of Metals and Alloys, Perseus Books, 2nd Revised Edition (1995)
- [8] P.G. Kevrekidis, The Discrete Nonlinear Schrödinger Equation: Mathematical Analysis, Numerical Computations and Physical Perspectives Springer-Verlag, Berlin (2009)
- [9] P.L. Freddolino, C.B. Harrison, Y. Liu and Y. Schulten, Nature Phys. **6**, 751 (2010)